Published in final edited form as:
Synapse. 2013 February ; 67(2): . doi:10.1002/syn.21617.

Targeting Presynaptic Norepinephrine Transporter in Brown Adipose Tissue: A Novel Imaging Approach and Potential Treatment for Diabetes and Obesity

M. REZA MIRBOLOOKI[*], **CRISTIAN C. CONSTANTINESCU**, **MIN-LIANG PAN**, and **JOGESHWAR MUKHERJEE**
Preclinical Imaging, Department of Radiological Sciences, University of California Irvine, Irvine, California

Abstract

Brown adipose tissue (BAT) plays a significant role in metabolism. In this study, we report the use of atomoxetine (a clinically applicable norepinephrine reuptake inhibitor) for ^{18}F-FDG PET imaging of BAT and its effects on heat production and blood glucose concentration. Fasted-male Sprague-Dawley rats were administered with intravenous ^{18}F-FDG. The same rats were treated with atomoxetine (0.1 mg/kg, i.v.) 30 min before ^{18}F-FDG administration. To confirm the β-adrenergic effects, propranolol (β-adrenergic inhibitor) 5 mg/kg was given intraperitoneally 30 min prior to atomoxetine administration. The effect of atomoxetine on BAT metabolism was assessed in fasted and non-fasted rats and on BAT temperature and blood glucose in fasted rats. In ^{18}F-FDG PET/CT images, interscapular BAT (IBAT) and other areas of BAT were clearly visualized. When rats were fasted, atomoxetine (0.1 mg/kg) increased the ^{18}F-FDG uptake of IBAT by factor of 24 within 30 min. Propranolol reduced the average ^{18}F-FDG uptake of IBAT significantly. Autoradiography of IBAT and white adipose tissue confirmed the data obtained by PET. When rats were not fasted, atomoxetine-induced increase of ^{18}F-FDG uptake in IBAT was delayed and occurred in 120 min. For comparison, direct stimulation of β_3-adrenreceptors in non-fasted rats with CL-316, 243 occurred within 30 min. Atomoxetine-induced IBAT activation was associated with higher IBAT temperature and lower blood glucose. This was mediated by inhibition of norepinephrine reuptake transporters in IBAT leading to increased norepinephrine concentration in the synapse. Increased synaptic norepinephrine activates β_3-adrenreceptors resulting in BAT hypermetabolism that is visible and quantifiable by ^{18}F-FDG PET/CT.

Keywords

atomoxetine; blood glucose; ^{18}F-FDG PET; Brown fat

INTRODUCTION

The presence of the brown adipose tissue (BAT) in rodents (Lachance and Page, 1953) and human neonates (Symonds et al., 2011) as well as adult humans (Cohade et al., 2003; Cypess et al., 2009; Nedergaard et al., 2007), and its role in metabolism has become an important area of investigation for obesity and diabetes. In addition to BAT being a major lipid-burning tissue, it has also been demonstrated as a major organ for glucose disposal (Nedergaard et al., 2011). Glucose uptake in BAT occurs via the two dominant isoforms of

[*]Correspondence to: M. Reza Mirbolooki, MD, PhD, Preclinical Imaging, Department of Radiological Sciences, University of California Irvine, Medical Sciences B, B-140, Irvine, CA 92697-5000, USA. rezam@uci.edu.

glucose transporters, GLUT1 (Shimizu et al., 1998) and GLUT4 (Santalucia et al., 1992), and is then metabolized producing heat. Long time exposure to cold temperature prior to PET is the only current method to study BAT in human, a function mediated by the β-adrenergic system (van Marken Lichtenbelt et al., 2009). Prevalence of BAT from these lowered temperature studies ranged from 30 to 95% in a small number of subjects (Pfannenberg et al., 2010; Saito et al., 2009; van Marken Lichten-belt et al., 2009), however, the difficulties involved with this method reduces the reliability of the imaging method (Au-Yong et al., 2009).

Thin unmyelinated fibers that contain norepinephrine are innervated in the brown adipocytes (De Matteis et al., 1998). In mature brown adipocytes, norepinephrine interacts with β-adrenergic receptors. β_2-adrenoceptors are not expressed in the brown adipocytes (Bengtsson et al., 2000). β_1-adrenoceptors are expressed in mature brown adipocytes, and coupled to cAMP production (Bronnikov et al., 1999), and in the absence of the β_3-adrenoreceptors, they enhance glucose uptake by increasing the synthesis of uncoupling protein-1, UCP1 (Mattsson et al., 2011). The β_3-adrenreceptor is the most studied for BAT metabolism, while known as a regulator of the metabolism of fatty acids (Bartelt et al., 2011) it also enhances glucose uptake both in vivo (Mirbolooki et al., 2011) and in vitro (Liu et al., 1998; Marette and Bukowiecki, 1991). It is believed that β_3-adrenreceptor enhances glucose uptake through augmentation of the synthesis of glucose transporters 1 and 4 (GLUT1/4) and their translocation to the cell membrane (Bartelt et al., 2011; Dallner et al., 2006) as well as overexpression of HK-II mRNA (Postic et al., 1994; Fig. 1). Currently, the total amount of BAT in the body does not seem to be large, yet it can potentially be a significant glucose-clearing organ. Direct effects of norepinephrine and β_3-adrenergic agonists on blood glucose level have been reported (Dallner et al., 2006; Liu et al., 1998; Marette and Bukowiecki, 1991), however, no study has reported the indirect effects of norepinephrine transporter (NET) inhibitors on glucose metabolism. In recent clinical trials, treatment of depression with antidepressant, milnacipran (serotonin and norepinephrine reuptake blocker), was associated with improvement in metabolic parameters including blood glucose level (Abrahamian et al., 2009). It remains unclear that either an improvement of depressive symptoms or the effects of the medication independently improved the metabolic parameters.

Atomoxetine, (−)-N-methyl-3-phenyl-3-(o-tolyloxy)-propylamine hydrochloride (formerly called tomoxe-tine or LY139603) is a potent and highly selective inhibitor of presynaptic NET that is used for treatment of attention-deficit/hyperactivity disorder (ADHD; Garnock-Jones and Keating, 2009); a common behavioral disorder found in 3–7% of school age children. Atomoxetine leads to increased synapse concentrations of norepinephrine and therefore an increase in adrenergic neurotransmission (Bymaster et al., 2002). Uptake of a highly selective NET ligand, ^{11}C-MRB ((S, S)-*O*-[^{11}C] methylreboxetine), suggests the existence of these transporters in BAT (Lin et al., 2012). We envision that atomoxetine may result in the enhancement of the BAT metabolism by increasing synapse concentrations of norepinephrine (Fig. 1). In this study, we report the enhancement of BAT metabolism by atomoxetine measurable with ^{18}F-FDG PET/CT and its blood glucose lowering effects.

MATERIALS AND METHODS

Animals

Male Sprague-Dawley rats, aged 8–10 weeks were used in this study. Rats were purchased from Charles River Laboratories (Wilmington, MA) and housed under controlled temperatures of 22°C ± 1°C, in a 12-h light–dark cycle, on at 6:00 AM, with water and food chow ad libitum. All animal studies were approved by the Institutional Animal Health Care and Use Committee of University of California-Irvine.

Equipments

An Inveon-dedicated PET scanner (Siemens Medical Solutions, Malvern, PA), which has a resolution of 1.46 mm in the center of the field-of-view, was used for the PET studies (Constantinescu and Mukherjee, 2009). An Inveon Multimodality (MM) CT scanner (Siemens Medical Solutions, Malvern, PA) was used for CT acquisitions in combined PET/CT experiments. All in vivo images were analyzed using PMOD Software (PMOD Technologies, Zurich, Switzerland) and Inveon Research Workplace (IRW) software (Siemens Medical Solutions, Malvern, PA). A Sigma Delta anesthetic vaporizer (DRE, Louisville, KY) was used to induce and maintain anesthesia during intravascular injections and PET/CT acquisitions. Slices of BAT were prepared using the Leica CM1850 cryotome (Leica Microsystems, Buffalo Grove, IL). Radioactivity was counted using CRC-15R dose calibrator (Cap-intec, Ramsey, NJ). Ex vivo ^{18}F-FDG labeled sections were exposed to phosphor films and scanned using the Cyclone Phosphor Imaging System (Packard Instruments, Meriden, CT) and analyzed using Opti-quant™ software. Temperatures were measured using a precalibrated thermometer probe TAT-2000C (Exergen, Watertown, MA). Blood glucose was measured by a glucometer (Contour, Bayer, Japan).

Chemicals

Atomoxetine and propranolol were purchased from Sigma-Aldrich (St. Louis, MO). CL-316, 243 was purchased from Tocris Bioscience (Bristol, UK). ^{18}F-FDG was purchased from PETNET solutions (Irvine, CA). Isoflurane was purchased from Clipper Distributing Company (St. Joseph, MO).

Experimental protocol

Static PET imaging on fasted animals—All rats were fasted for at least 17 h before ^{18}F-FDG administration. On day one, rats (n = 3, Wt: 194 ± 5.3 g) were injected with normal saline (0.15 mL) through tail vein 30 min before intravenous (iv) administration of ^{18}F-FDG under 2% isoflurane anesthesia. They were awake between the injections and eventually were placed in the supine position in a rat holder and anesthetized with 2% isoflurane for upper-body PET imaging. The rat holder was placed on the PET/CT bed and 30 min-long PET scans were acquired 60 min after ^{18}F-FDG injections. All animals had a CT scan after the PET scan for attenuation correction and anatomical delineation of PET images. Four days later, the same rats (n = 3, Wt: 213 ± 8.1 g) were pretreated with 0.1 mg/kg atomoxetine (0.15 mL, iv) 30 min before ^{18}F-FDG administration. Experiments using propranolol preadministration were done on the same rats (n = 3, Wt: 230 ± 11.7 g), 4 days later, to evaluate whether enhanced ^{18}F-FDG uptake in activated BAT could be reduced. Propranolol 5 mg/kg (0.2 mL) was given, intraperitone-ally, 30 min prior to atomoxetine administration. The same method of injection of ^{18}F-FDG was used for all rats, as was the recovery period and re-anesthetization for PET (Fig. 2A).

Static PET imaging on non-fasted animals—Different rats were used for this experiment and were not fasted before ^{18}F-FDG administration. On day one, rats (n = 3 Wt: 324 ± 7.2 g) were injected with normal saline (0.15 mL) through tail vein 30 min before i.v. administration of ^{18}F-FDG. Four days later, the same rats (n = 3, Wt: 358 ± 25.4 g) were pre-treated with 0.1 mg/kg atomoxetine (0.15 mL, iv) 30 min before ^{18}F-FDG administration (Fig. 2B). Uptake of ^{18}F-FDG in non-fasted animals was compared using either atomoxetine or the selective β_3-adrenoreceptor agonist, CL-316, 243. First, the total of three rats were injected with either normal saline or CL-316, 243, on different days, through tail vein, and 30 min before i.v. administration of ^{18}F-FDG (Fig. 2C). Next, three other rats were injected with either normal saline or atomoxetine (0.1 mg/kg), on different days, through tail vein, and 120 min before i.v. administration of ^{18}F-FDG (Fig. 2D). The same

method of injection of ^{18}F-FDG was used for all rats, as was the recovery period and re-anesthetization for PET.

Dynamic PET imaging on fasted animals—All rats were fasted for at least 17 h before PET acquisition. On day one, rats (n = 3, Wt: 425 ± 40 g) were injected with normal saline (0.15 mL) through tail vein 30 min before PET data acquisition and then were placed in the supine position in a rat holder and anesthetized with 2% isoflurane for upper-body PET imaging. The rat holder was placed on the PET/CT bed and 120 min-long PET scans were acquired followed by a 10-min CT scan. The CT scan was used for attenuation correction and anatomical delineation of PET images. Intravenous administration of ^{18}F-FDG was done through tail vain just after the start of PET data acquisition. Two days later, the same rats (n = 3, Wt: 422 ± 38 g) were pretreated with 0.5 mg/kg i.v. atomoxetine 30 min before PET data acquisition (Fig. 2E) under the same protocol.

PET/CT imaging

The Inveon PET and MM CT scanners were placed in the “docked mode” for combined PET/CT experiments. All images were calibrated in units of Bq/cm^3 by scanning a Ge-68 cylinder (6 cm diameter) with known activity and reconstructing the acquired image with parameters identical to those of ^{18}F-FDG images. PET data acquisition was followed by a 10-min CT scan (large area detector, 10 cm × 10 cm field-of-view) for attenuation correction and anatomical delineation of PET images. The PET images were spatially transformed to match the reconstructed CT images. PET images were corrected for random coincidences, attenuation and scatter. The CT projections were acquired with the detector-source assembly rotating over 360 degrees and 720 rotation steps. A projection bin factor of 4 was used to increase the signal-to-noise ratio in the images. The CT images were reconstructed using cone-beam reconstruction with a Shepp filter with cutoff at Nyquist frequency and a binning factor of two resulting in an image matrix of 480 × 480 × 632 and a voxel size of 0.206 mm.

Static PET imaging protocol—After 60 min of ^{18}F-FDG uptake, rats were anesthetized and positioned in the supine position with their chest, neck, and head within the field-of-view of the PET scanner. PET data were acquired for 30 min. The data were reconstructed as 128 × 128 × 159 matrices with a transaxial pixel of 0.776 mm and slice thickness of 0.796 mm using a OSEM3D/Fast MAP algorithm (2 OSEM3D iterations, 18 MAP iterations, 0.1 smoothing factor).

Dynamic PET imaging protocol—PET data were acquired for 120 min. The data were reconstructed as 128 × 128 × 159 matrices with a transaxial pixel of 0.776 mm and slice thickness of 0.796 mm using a OSEM3D/Fast MAP algorithm (2 OSEM3D iterations, 18 MAP iterations, 0.1 smoothing factor). The reconstructed time frames were 5 s during the initial 3 min, 20 s during 3–5 min, 30 s during 5–10 min, 60 s during 10–30 min, and 300 s each for the rest of the scan, resulting in a total of 90 frames.

Image analysis

The magnitude of BAT ^{18}F-FDG activation was expressed as standard uptake value (SUV), which was computed as the average ^{18}F-FDG activity in each volume of interest, VOI (in kBq/mL) divided by the injected dose (in MBq) times the body weight of each animal (in kg) (Benz et al., 2012; Letovanec et al., 2012; Marnane et al., 2012). For quantitative analysis, VOIs were drawn on PET images for inter-scapular BAT (IBAT) and on CT images for interscapular white adipose tissue (IWAT) and muscle (Biceps Brachii) using PMOD. Similarly to previously described methods (Schinagl et al., 2011), the VOIs were first delineated visually by contouring the ^{18}F-FDG activity that was clearly above normal background activity when rats treated with atomoxetine (Fig. 3A). PET SUV and CT HU of

BAT increases under activated conditions (Baba et al., 2010). After visually delineating the VOIs, the SUV and HU levels were thresholded to maximize the difference between IBAT and IWAT (Fig. 4). The same VOIs were applied on the images obtained from the same rats in both normal saline and propranolol treatments.

Kinetic modeling—Volume-of-interests (VOIs) were manually delineated around IBAT in the reconstructed dynamic PET images of atomoxetine treated. Before kinetic modeling, a semi-quantitative measure (SUV) was calculated to compare intra-group time activity curves (TAC) and particularly differences in TACs between control and atomoxetine-treated animals. The TAC in each BAT VOIs was fitted to a four-parameter two-tissue compartment kinetic model that describes the distribution and uptake of ^{18}F-FDG in tissue using an image-derived input function (IDIF) computed for each animal (Roe et al., 2010). A Marquardt optimization algorithm with 200 iterations was used for non-linear fitting and Poisson weighting. Compartmental analysis was performed with the PMOD kinetic modeling toolbox. A fixed tissue blood volume of 0.05 was used. The runs test was used for evaluating the goodness of fit. The kinetic rate constants K_1, k_2, k_3, and k_4 were estimated. The ^{18}F-FDG rate constant K_1 (mL/min/g) and k_2 (min^{-1}) are mediated by glucose transporters across cytomembranes, and k_3 (min^{-1}) and k_4 (min^{-1}) represent phosphorylation by hexokinase and dephosphorylation by glucose-6-phosphatase, respectively (Mizuma et al., 2010). The FDG influx constant, K_i, was computed as $K_i = K_1 \times k_3/(k_2 + k_3)$. The regional BAT glucose metabolic rate (rBMRglu) was calculated using K_i, the measured blood glucose concentration for each animal (Glu) and a lumped constant (LC) of 1.14 (Vanttinen et al., 2005), with the formula rBMRGlu = $K_i \times$ Glu/LC.

The input function was computed for each animal using a reported procedure (Roe et al., 2010). The first minute time frames were summed and a seed region with highest activity was identified in the left ventricle. One-minute time activity curves with the highest peak to the plateau ratio (>4) were extracted and then averaged. The interval between the peak-time and 1 min of resulting curve was fitted to a bi-exponential curve $[A_{exp}(-Bt) + C_{exp}(-Dt)]$ with a trust-region reflective algorithm using Matlab. The input function was then calculated from the actual data and the bi-exponential fit.

Dynamic SUV curves for the kinetics of ^{18}F-FDG were derived from the total SUV observed in the IBAT with and without pretreatment with atomoxetine (0.5 mg/kg). The ^{18}F-FDG clearance rates (k_{off}) from IBAT were measured, as previously described (Mukherjee et al., 1997), by plotting time vs. ln X/X_{30}, where X_{30} is the SUV of ^{18}F-FDG at time 30 and X is the SUV of ^{18}F-FDG at various times past X_{30}. The ^{18}F-FDG clearance rate was the slope of this plot and half-times ($T_{1/2}$) were computed using the equation, $T_{1/2} = 0.693/k_{off}$.

Autoradiography

For autoradiography, rats were treated similar to Figure 2A protocol. The only difference was that the rats were killed at 120 min and their IBAT and IWAT were harvested ($n = 3$, each group). Transverse sections obtained from the soft tissue of the interscapular brown adipose tissue (IBAT) region at the level of T5 were frozen on dry ice to provide 60-μm-thick slides for autoradiography. Slides were exposed to phosphor screens for 1 h and scanned using the Cyclone Plus storage phosphor system. The acquired image was then analyzed with OptiQuant™ software where data in each region of interest (ROI) were quantified in digital light units per mm^2 (DLU/mm^2).

Intravenous glucose tolerance test

After at least 17 h of fasting, an intravenous glucose tolerance test (IVGTT) was performed to determine the glucose clearance rate for up to 60 min ($n = 4$). A bolus of glucose (0.5 g/kg in a 50% saline solution) was given within 30 s into the tail vein. The second IVGTT, 2 days apart from the first one, was performed on the same rats. A bolus of atomoxetine (0.5 mg/kg) was given through the tail vein at 10 min prior to IVGTT. Blood was sampled from the saphenous vein at −10, 0, 2, 5, 15, 30, 45, and 60 min for assessment of the blood glucose. The blood glucose clearance rate (G_c) was determined in three phases including: phase 1: fast clearance (minutes 2–5); phase 2: moderate clearance (minutes 5–30); phase 3: slow clearance (minutes 30–60) using the following formula:

$$G_c = \frac{(G_{t1} - G_{t0})}{G_{t0} \times (t1 - t0)}$$

where G_{t0} is blood glucose level at the beginning of the phase; G_{t1} is blood glucose level at the end of the phase; $t0$ is time when the phase begins; and $t1$ is time when the phase ends. The value of G_c was expressed as % min^{-1}

Temperature measurement

IBAT temperatures were measured using a precalibrated thermometer probe placed on the skin in the interscapular area. The hair was removed from the upper back of the rats with NAIR® hair removal lotion containing sodium hydroxide (Church & Dwight, Princeton, NJ) 1 day prior to the experiment. IBAT temperature was monitored during a period of 1 min to obtain a stable measure. Rats ($n = 4$) were awake during measurements. Baseline IBAT temperatures were measured prior to i.v. administration of atomoxetine. Temperatures were measured again 30 and 60 min after atomoxetine injection.

Photomicrograph production

All original in vivo images were obtained either using PMOD Software (PMOD Technologies, Zurich, Switzerland) or Inveon Research Workplace (IRW) software (Siemens Medical Solutions, Malvern, PA). The autoradiography images were obtained using OptiQuant™ software. The original images were then inserted and sorted in Microsoft Powerpoint 2010 to produce final images which then were saved as. TIFF files. No modifications to contrast or brightness was done.

Statistical analysis

Statistical differences between groups were determined using either paired or independent Student's *t*-test or one way ANOVA with a Bonferroni post hoc test in SPSS statistical software, version 16.0 for Windows (Chicago, IL). Statistical tests like the paired *t*-test are mathematically more powerful for a given sample size than are unpaired tests because in paired tests, each measurement is matched with its own control (Eng, 2003). In our study, individual rats were imaged on multiple occasions so that they could serve as their own control. We calculated the statistical power with Pairwise Sample method and based on IBAT SUV data, it was equal to 1.0. A *P*-value of <0.05 was considered to indicate statistical significance.

RESULTS

Targeting presynaptic NET to visualize BAT by ^{18}F-FDG PET

Treatment of rats with atomoxetine (0.1 mg/kg) at ambient temperature increased the total ^{18}F-FDG uptake of all regions of BAT. Activated interscapular, cervical, periaortic, and intercostal BATs were clearly observed in 3-dimentional analysis of ^{18}F-FDG PET/CT images and regions confirmed anatomically by CT coregistration (Fig. 3B). This regional distribution was consistent among different rats treated with atomoxetine. In control rats, the order of ^{18}F-FDG uptake was similar, but with lower intensities. Smaller areas such as the intercostal BAT was difficult to discern under control conditions. We chose to compare IBAT uptakes between the groups due to its more consistent shape described previously (Mirbo-looki et al., 2011).

Effect of atomoxetine on ^{18}F-FDG Uptake in BAT when animals are fasted

PET/CT images revealed intense ^{18}F-FDG uptake in IBAT of atomoxetine treated rats at ambient temperature (Fig. 5A). The effect of increased ^{18}F-FDG was consistent across animals treated with atomoxetine. Treatment of rats with atomoxetine (0.1 mg/kg) at ambient temperature, 30 min before ^{18}F-FDG administration, increased the total ^{18}F-FDG SUV of IBAT to 11.8 ± 5.8, which is about 24-fold greater ($P < 0.001$) when compared with ^{18}F-FDG SUV in untreated rats of 0.5 ± 0.2 (Fig. 5B). This high level of ^{18}F-FDG SUV in IBAT induced by atomoxetine was decreased dramatically by preinjection of propranolol (reduced by 89.5% to 1.2 ± 1.0, $P < 0.001$). Reduction in the levels of ^{18}F-FDG SUV in the propranolol treated group confirms that the atomoxetine effect is through β-adrenoreceptor. There was no significant difference in IWAT and muscle uptakes between groups (Table I).

IBAT isolated from control, atomoxetine, and atomoxetine–propranolol combination treated rats had distinct features as seen in Figure 6. This BAT area in atomoxetine-treated animals had significant amounts of ^{18}F-FDG uptake as seen in autoradiographic images of the transverse sections obtained from the IBAT region. The quantitative data of autoradiography measures in IBAT and WAT regions are summarized in Table II.

Effect of atomoxetine on ^{18}F-FDG uptake in BAT when animals are not fasted

Under non-fasting conditions, PET/CT images revealed low ^{18}F-FDG uptake in IBAT of atomoxetine (0.1 mg/kg) treated rats when it was administered 30 min prior to ^{18}F-FDG administration at ambient temperature (Fig. 7). In atomoxetine pretreated non-fasted rats, ^{18}F-FDG SUV of IBAT was 1.7 ± 1.4 when compared with that of untreated rats (1.0 ± 0.5, NS). There was no significant difference in IWAT and muscle uptakes between groups (Table III). Compared to fasted rats, the IBAT ^{18}F-FDG uptake in non-fasted rats at 30 min post atomoxetine injection was lower. Blood glucose levels were measured twice prior to atomoxetine and ^{18}F-FDG administrations. Blood glucose was significantly higher prior to atomoxetine administration in non-fasted when compared with fasted rats (155 ± 22.0 vs. 101 ± 27.7 mg/dL, $P < 0.04$). Prior to ^{18}F-FDG administration, blood glucose was still higher in non-fasted rats, however, the difference was not significant (143 ± 11.6 vs. 109 ± 26.6 mg/dL, $P < 0.09$). We did not observe hypoglycemia (blood glucose below 70 mg/dL) neither in fasted nor in non-fasted rats after administration of atomoxetine.

Longer blocking of the NET in non-fasted rats with atomoxetine (0.1 mg/kg, 120 min before ^{18}F-FDG administration) at ambient temperature increased the total ^{18}F-FDG SUV of IBAT to 4.1 ± 1.8 (Fig. 7) when compared with 1.7 ± 1.4 ($P < 0.05$) at 30 min before ^{18}F-FDG administration. There was no significant difference in IWAT and muscle uptakes between groups. Since the level of norepinephrine is significantly lower when animals are

not fasted (Jensen et al., 1987), our data suggest that longer time is required for enough norepinephrine accumulation in the synapse to activate BAT. Direct stimulation of β_3-adrenreceptors in non-fasted rats with selective β_3- receptor agonist, CL-316, 243 (0.1 mg/kg), at ambient temperature, 30 min before ^{18}F-FDG administration, increased the total ^{18}F-FDG SUV of IBAT to 14.0 ± 2.9 (Fig. 7) when compared with ^{18}F-FDG SUV in untreated rats of 1.6 ± 0.7.

Quantitative kinetic modeling and atomoxetine effect assessment

After correcting for injected dose of ^{18}F-FDG and body weight of the rats, different shapes of the TACs were obtained in IBAT of atomoxetine-treated when compared with untreated rats (Fig. 8A). Significant differences were detected both in the initial phase of the ^{18}F-FDG uptake (t_{2min}, $P = 0.018$; t_{10min}, $P = 0.040$; t_{20min}, $P = 0.046$; t_{30min}, $P = 0.012$) and at the end of the dynamic scan (t_{90min}, $P = 0.007$; t_{100min}, $P = 0.003$; t_{110min}, $P = 0.001$; t_{120min}, $P = 0.001$). Kinetic modeling allowed quantification of the kinetic parameters K_1, k_2, k_3, k_4, K_i, and rBMRGlu in IBAT. All kinetic parameters (with the exception of k_4) of the IBAT in atomoxetine treated rats were larger than those in untreated rats. Kinetic evaluation showed 1.5-fold increase in ^{18}F-FDG transport (ATX; $K_1 = 0.128 \pm 0.021$ min^{-1}vs. control; $K_1 = 0.087 \pm 0.035$ min^{-1}, $P = 0.077$) and 3.6-fold increase in hexokinase activity (ATX; $k_3 = 0.143 \pm 0.100$ min^{-1} vs. control; $k_3 = 0.031 \pm 0.029$ min^{-1}, $P = 0.067$) in the IBAT. No significant difference was observed in the average of kinetic parameters k_2 and k_4 of the IBAT between untreated rats ($k_2 = 0.026 \pm 0.026$ min^{-1}, and $k_4 = 0.006 \pm 0.005$ min^{-1} and atomoxetine-treated rats $k_2 = 0.096 \pm 0.080$ min^{-1}, and $k_4 = 0.001 \pm 0.003$ min^{-1}). IBAT net influx rate constant (K_i) for the glucose was significantly larger in atomoxetine-treated rats (0.079 ± 0.016 vs. 0.047 ± 0.017 min^{-1}, $P = 0.038$). The kinetic modeling also displayed a significant increase in FDG uptake in the IBAT of atomoxetine-treated rats when compared with the IBAT of control rats (ATX; rBMRGlu 35.5 ± 8.7 μmol/min/100 g vs. control; rBMRGlu 16.8 ± 7.1 μmol/min/100 g, $P = 0.046$). Clearance of ^{18}F-FDG from IBAT in the absence of atomoxetine was rapid ($T_{1/2} = 147$ min) with a clearance rate constant of 4.7×10^{-3} min^{-1} while that with atomoxetine was significantly slower ($T_{1/2} = 462$ min, $P = 0.026$) with a clearance rate constant of 1.5×10^{-3} min^{-1} (Fig. 8B).

Effect of atomoxetine on blood glucose and brown adipose tissue temperature

Data from Intravenous Glucose Tolerance Test (IVGTT) revealed that blood glucose level was significantly lower when the rats were treated with atomoxetine (127 ± 18.7 vs. 208 ± 31.2 mg/dL, $P < 0.005$) at 30 min after glucose administration and remained significantly lower thereafter (Fig. 9A). The blood glucose clearance rate was significantly faster during phase 2 when the rats were treated with atomoxetine when compared with control (1.9 ± 0.3 vs. 0.6 ± 0.4%min^{-1}, $P < 0.001$). However, no significant changes were observed in phases 1 and 3 after treatment with atomoxetine (Fig. 9B). Temperature rise is a key outcome of BAT activity. The temperature of the IBAT region increased when rats were treated with atomoxetine. Treatment of rats with atomoxetine (0.1 mg/kg) at ambient temperature increased the IBAT temperature from the baseline of 99.4 ± 0.1 to 99.6 ± 0.4°F ($P < 0.5$) at 30 min and to 100.2 ± 0.2°F at 60 min ($P < 0.01$) post atomoxetine injection, which is about one degree warmer when compared with IBAT temperature of the rats when untreated (Fig. 9C).

DISCUSSION

The first major finding of the current study is that NET blocker, atomoxetine, augments ^{18}F-FDG uptake of BAT through β-adrenergic receptors under fasting conditions. This augmentation occurs at room temperature and within 30 min after drug administration. Therefore, this approach could be used to visualize BAT with ^{18}F-FDG PET imaging not

only in animal models to study brown adipocyte biology, but also in humans for BAT prevalence studies. Large retrospective studies report that the prevalence of detected BAT in the patients is 3–5% (Au-Yong et al., 2009; Cypess et al., 2009; Kim et al., 2008; Stefan et al., 2009). This extremely low prevalence of BAT in the adult population reduces its potential significance for adult human metabolism. However, a major problem with these retrospective studies is that only the prevalence of activated BAT in patients with a diagnosed disease has been reported. BAT is only active when its thermogenic function is required (Cannon and Nedergaard, 2004). Since ^{18}F-FDG uptake is a direct consequence of tissue activity (Inokuma et al., 2005) inactive BAT would not be visible on PET scans.

The logical step is to actively stimulate BAT so that ^{18}F-FDG uptake would be consistent across the subjects. Long time exposure to cold temperature prior to PET is the only current method to study BAT in human, a function mediated by the β-adrenergic system (van Marken Lichtenbelt et al., 2009). Individuals need to remain in a room with a temperature around 61°F with light clothing for about 2 h prior to PET imaging. Additionally, one foot would intermittently be placed into a bucket filled with ice-cold water. The BAT prevalence from these studies ranged from 30 to 95% (Pfannenberg et al., 2010; Saito et al., 2009; van Marken Lichtenbelt et al., 2009), which is higher than those of the retrospective studies. However, the difficulty of this method is the huge range of prevalence due to the variations in sympathetic responses to low temperature in different individuals, and in different seasons in one individual (Au-Yong et al., 2009), which reduces the reliability of the imaging method in addition to the required discomfort introduced by the cold exposure. We believe that the pharmacologic approach reported in this study is highly translational to clinic for two main reasons. First, atomoxetine is a selective norepinephrine reuptake inhibitor and has low abuse potential (Garnock-Jones and Keating, 2009). Atomoxetine is a phenoxypropylamine derivative and is structurally related to the antidepressant fluoxetine (Scherer et al., 2009). The common side effects reported with the use of atomoxetine include “headache, abdominal pain, nausea, vomiting, decreased appetite, weight loss, irritability, insomnia, and sedation” (Ledbetter, 2006). Cardiovascular side effects are less commonly reported (Habel et al., 2011). Atomoxetine cardiovascular side effects reported in adult placebo-controlled trials have included increased heart rate (3.0%), and increased blood pressure. In adult placebo-controlled trials, the mean increase in heart rate was reported as 5 beats/min and the mean increase in blood pressure was reported as 3 mm Hg systolic and 1 mm Hg diastolic (Adler et al., 2005). These side effects are negligible since they are less severe than the effects of a simple exercise. It has been used in psychiatry for the treatment of both adult and pediatric ADHD with relatively benign side effects (Michelson et al., 2003; Rosler et al., 2010). Second, under fasting conditions, atomoxetine-initiated extensive ^{18}F-FDG uptake in BAT (by a factor of 24) comparable to that observed with cold exposure in human supraclavicular area (by a factor of 15; Virtanen et al., 2009).

Although there are no such direct studies to date, it is generally admitted that adrenergic agonists had to increase human BAT activity (Nedergaard et al., 2010). BAT in patients with pheochromocytoma (excess release of epinephrine and norepinephrine from adrenal gland) has been reported to exhibit very intense ^{18}F-FDG uptake (Iyer et al., 2009; Yamaga et al., 2008). Any potential agonist had to be highly specific for β_3-adrenoreceptors otherwise their interaction with β_1- and β_2-adrenoreceptors may lead to serious cardio- vascular side effects (Zelinka et al., 2012). CL-316, 243 is a drug with a high selectivity for the β_3-adrenoreceptor. Binding affinity of CL-316, 243 is low for the β_1- and β_2-ARs, thus exhibiting a 10,000-fold selectivity (binding affinities of CL-316, 243: K_i: $\beta_1 \geq 100$ μM; $\beta_2 = 30$ μM; $\beta_3 = 3$ nM; Bloom et al., 1992; Yoshida et al., 1994). Recently, we reported activated BAT in rodents with CL-316, 243 (Mirbolooki et al., 2011). Because of the selective nature of CL-316, 243, the increase in ^{18}F-FDG uptake is due to the direct stimulation of the β_3-adrenoreceptors. Although its in vitro binding to the human β_3-adrenoreceptor is identical to

that of the rodent receptor, in contrast to the rodent receptor, where CL-316, 243 is a full agonist, it is only a partial (60%) agonist at the human β_3-adrenoreceptor and its bioavailability is poor, with ~10% of an oral dose being absorbed (Weyer et al., 1998).

The role of BAT in metabolism has been underappreciated due to the aforementioned limitations. Applying atomoxetine in BAT ^{18}F-FDG PET imaging may help understand if BAT activity could potentially be an important part of metabolic control in the adult humans. Atomoxetine is a potent inhibitor of the presynaptic NE transporter and has minimal affinity for other neuro-transmitter transporters and neuronal receptors. Binding affinity of atomoxetine is low for the human DAT and SERT (K_i: DAT ≥1457 nM; SERT = 77 nM; NET = 5 nM; other neurotransmitter transporters > 1 μM; Bymaster et al., 2002). It also has a low affinity for post-synaptic receptors for all neurotransmitters, including NA. ATX therefore has a longer duration of action. It has high aqueous solubility and biological membrane permeability that facilitates its rapid and complete absorption after oral administration. Its absolute oral bioavailability ranges from 63 to 94% (Sauer et al., 2005). Selective nature of atomoxetine in blocking norepinephrine reuptake transporters and the increase in ^{18}F-FDG uptake is due to the indirect stimulation of the β-adrenoreceptors. This increase is substantially higher than that of previously reported pharmacological challenge studies using nicotine and ephedrine (Baba et al., 2007). Propranolol, a nonselective β-blocker, inhibits atomoxetine-induced BAT activation to control levels and confirmed the likelihood of action of it via the β_3-adrenoceptors (the most dominant adrenoreceptor in BAT). This is the first study reporting the use of atomoxetine to visualize BAT with ^{18}F-FDG PET imaging. The current FDA approval status and known clinical experience with this molecule accelerates translation of this promising animal data into human investigation. There are few reports introducing atomoxetine as a weight loss agent. A preliminary study to evaluate short-term anti-obesity efficacy of atomoxetine demonstrated modest short-term weight loss in obese women (Gadde et al., 2006). In a trial on outpatients with binge-eating disorder, atomoxetine was also found to be efficacious (McElroy et al., 2007). However, it was not effective for weight loss in those who have gained weight on either clozapine or olanzapine (Ball et al., 2011). The mechanisms of action of atomoxetine have been explained mostly through the central nervous system (CNS).

A standard ^{18}F-FDG PET/CT is done under fasting conditions due to glucose competition effects (Fueger et al., 2006). Compared to fasted rats, the low IBAT ^{18}F-FDG uptake in non-fasted rats at 30 min post atomoxetine injection was possibly due to the following reasons: (1) higher blood glucose concentration in non-fasted rats decreased the rate of ^{18}F-FDG accumulation by competition (Burrows et al., 2004) or; (2) nor-epinephrine concentration is lower when rats are not fasted (Jensen et al., 1987), therefore, short time blocking of NET did not result in a quick increase of norepinephrine and stimulation of β-adrenreceptors. To rule out the first hypothesis, blood glucose levels were measured. Blood glucose was significantly higher prior to atomoxetine administration in non-fasted when compared with fasted rats, however, prior to ^{18}F-FDG administration there was no significant difference in blood glucose levels between non-fasted and fasted rats. To investigate the second hypothesis, longer NET-blocking experiments and direct stimulation of β_3-adrenreceptors were performed. No significant difference in blood glucose levels at the time of ^{18}F-FDG administration between fasted and non-fasted rats suggests that blood glucose concentration is less likely the reason of low IBAT ^{18}F-FDG uptake in short-time exposure to atomoxetine in non-fasted rats. On the other hand, low ^{18}F-FDG uptake of the IBAT with short-term NET blocking (atomoxetine 30 min before ^{18}F-FDG injection) and high ^{18}F-FDG uptake with long-term NET blocking (atomoxetine 120 min before ^{18}F-FDG injection) and direct stimulation of β_3-adren-receptor (CL-316, 243) suggest that low norepinephrine levels in non-fasted rats is more likely the reason of low IBAT ^{18}F-FDG uptake in short-time exposure to atomoxetine in non-fasted rats.

One may argue not use of female rats as a limitation of this study. We agree with this, however, female rats have higher levels of UCP-1 in the IBAT depot when compared with males when housed at the same temperature (Quevedo et al., 1998), suggesting that their BAT is more active than males. There are plenty retrospective studies that active BAT is more often detected in females than in males (Au-Yong et al., 2009; Cheng et al., 2009; Kim et al., 2008). However, when BAT was actively stimulated, no difference in the prevalence between the sexes was found (Saito et al., 2009; Yoneshiro et al., 2011).

The second major finding of the current study is that, when compared with control, atomoxetine-treated rats had higher rBMRGlu in IBAT because of increased GLUT and HK activities, which is suggested by an increase in both K_1 and k_3 values (Fig. 10). BAT presents a dense sympathetic innervation and its metabolic activity is regulated by β_3 and α_2 receptors. Activation of β_3 receptors increases and activation of α_2 receptors decreases perfusion and metabolic activity. Norepinephrine binds to both types of receptors, but its effect on β_3 receptors is predominant and norepinephrine markedly stimulates metabolic activity (Lafontan and Berlan, 1993). These results were consistent with previous reports on the effects of norepinephrine on GLUT and HK expressions in BAT: Shimizu et al. (1998) reported that norepinephrine stimulated glucose transport in brown adipocytes by enhancing the functional activity of GLUT1 through a cAMP-dependent mechanism; Chernogubova et al. (2004) reported that norepinephrine signaled translocation of GLUT4 through the classical insulin pathway from PI3K in addition to cAMP effect on GLUT1; Postic et al. (1994) reported that GLUT-4 and HK-II mRNA were increased twofold to fourfold in BAT of rats exposed to cold (20°C) when compared with rats maintained at 37°C. Cold is known to activate BAT through sympathetic pathway (Cypess et al., 2012).

The effect of atomoxetine on ^{18}F-FDG IBAT SUV in the static scans was significantly greater than in the dynamic scans. For the dynamic scans, the animals were under isoflurane anesthesia throughout the uptake period, unlike the static scans where the animals were awake. Isoflurane anesthesia has been reported to markedly reduce ^{18}F-FDG uptake by BAT (Hildebrandt et al., 2008). Keeping the animal under isoflurane anesthesia for the whole uptake period not only minimizes ^{18}F-FDG uptake by BAT but also decreases blood clearance resulting in higher activity concentrations in liver and kidneys (Fueger et al., 2006). Effect of isoflurane on the kinetic parameters of ^{18}F-FDG uptake in IBAT in our dynamic experiments is unclear. It is possible that differential effects of anesthesia on GLUT1/GLUT4 and hexokinase might affect kinetic parameters.

We believe that kinetic parameters in this study provided valuable biological information explaining the differences in ^{18}F-FDG uptake, by taking underlying pharmacokinetic mechanisms into account. However, the data had to be interpreted using caution due to certain limitations. Studies on kinetic modeling often involve estimation of a mean arterial input function from repeated arterial blood sampling. This procedure is technically challenging in small animals, and is also limited by the small volume of blood that can be withdrawn without affecting these small animals' physiological function. In our study, both IBAT and heart were in the field-of-view simultaneously, allowing individual input function to be derived from images. However, a shortcoming in our study is that our IDIFs have not been compared to results from arterial blood sampling for the baseline and atomoxetine experiments. Verification of the validity of the IDIFs is currently under investigation.

The third major finding of the current study is that atomoxetine increases BAT temperature and accelerates high blood glucose clearance. Animal studies have suggested an inevitable role of BAT in the development of obesity, insulin resistance, and diabetes (Hamann et al., 1996). The substrate for activated BAT consists predominantly of fatty acids and during activation, approximately 10% of the total BAT metabolism is derived from glucose uptake

(Ma and Foster, 1986). This is the first study reporting the use of atomoxetine as a BAT activator and a potential glucose lowering agent. Data reported in this study along with other observations support the notion that atomoxetine might be effective in the treatment of diabetes and obesity. There are a few studies showing glucose metabolism enhancements with inhibiting norepinephrine reuptakes, however, their mechanisms of action remains unclear. In a case of akinetic mutism, treatment with atomoxetine for a period of 8 weeks led to an increase in cerebral glucose metabolism in both the premotor and visual association cortices (Kim et al., 2010). Sibutramine is a combined norepinephrine and serotonin reuptake inhibitor. It is used as an antiobesity agent to reduce appetite and promote weight loss in combination with diet and exercise. It improves insulin resistance and glucose metabolism, however, it is believed that most of these effects resulting from weight loss rather than from an intrinsic effect of the drug (Scheen, 2010). Milnacipran is another serotonin norepinephrine reuptake inhibitor antidepressant. It has been used in comorbid depression, which is common in patients with diabetes mellitus. It improves blood glucose and HbA1C levels in type 2 diabetics. It is suggested that the effective treatment of depression results in higher sense of self-care, which lead to improvement in the metabolic parameters (Abrahamian et al., 2009). The data presented in this article suggest that BAT uptake is protective against hyperglycemia. This result reinforces the observation that BAT is a dedicated glucose uptake organ (Bartelt et al., 2011); and ^{18}F-FDG PET is useful for the development of new treatments for diabetes (Jacene et al., 2011).

CONCLUSION

The ability to visualize and quantify glucose metabolism in BAT on FDG PET/CT has significant implications. It may be used as a non-invasive in vivo imaging tool to study the role of BAT and to develop new treatments for diabetes and obesity. Atomoxetine increased net influx of glucose in IBAT. Further studies in diabetic and obese animal models are needed to observe its efficacy on metabolic parameters to ascertain its potential as an antidiabetic or antiobesity agent. These findings may support a novel approach of NET inhibitors as potential antiobesity or antidiabetic agents in addition to their current clinical use for ADHD.

Acknowledgments

The project described was supported by the National Institute of Diabetes and Digestive and Kidney Diseases with award numbers RC1DK087352 and R21DK092917. We thank Drs. George Chandy, Ping Wang and Albert Sun for helpful discussions.

References

Abrahamian H, Hofmann P, Prager R, Toplak H. Diabetes mellitus and co-morbid depression: Treatment with milnacipran results in significant improvement of both diseases (results from the Austrian MDDM study group). Neuropsychiatr Dis Treat. 2009; 5:261–266. [PubMed: 19557120]

Adler LA, Spencer TJ, Milton DR, Moore RJ, Michelson D. Long-term, open-label study of the safety and efficacy of atomoxetine in adults with attention-deficit/hyperactivity disorder: An interim analysis. J Clin Psychiatry. 2005; 66:294–299. [PubMed: 15766294]

Au-Yong IT, Thorn N, Ganatra R, Perkins AC, Symonds ME. Brown adipose tissue and seasonal variation in humans. Diabetes. 2009; 58:2583–2587. [PubMed: 19696186]

Baba S, Jacene HA, Engles JM, Honda H, Wahl RL. CT Hounsfield units of brown adipose tissue increase with activation: Preclinical and clinical studies. J Nucl Med. 2010; 51:246–250. [PubMed: 20124047]

Baba S, Tatsumi M, Ishimori T, Lilien DL, Engles JM, Wahl RL. Effect of nicotine and ephedrine on the accumulation of ^{18}F-FDG in brown adipose tissue. J Nucl Med. 2007; 48:981–986. [PubMed: 17504863]

Ball MP, Warren KR, Feldman S, McMahon RP, Kelly DL, Buchanan RW. Placebo-controlled trial of atomoxetine for weight reduction in people with schizophrenia treated with clozapine or olanzapine. Clin Schizophr Relat Psychoses. 2011; 5:17–25. [PubMed: 21459735]

Bartelt A, Bruns OT, Reimer R, Hohenberg H, Ittrich H, Peldschus K, Kaul MG, Tromsdorf UI, Weller H, Waurisch C, Eychmuller A, Gordts PL, Rinninger F, Bruegelmann K, Freund B, Nielsen P, Merkel M, Heeren J. Brown adipose tissue activity controls triglyceride clearance. Nat Med. 2011; 17:200–205. [PubMed: 21258337]

Bengtsson T, Cannon B, Nedergaard J. Differential adrenergic regulation of the gene expression of the beta-adrenoceptor subtypes beta1, beta2 and beta3 in brown adipocytes. Biochem J. 2000; 347(Pt 3):643–651. [PubMed: 10769166]

Benz MR, Czernin J, Allen-Auerbach MS, Dry SM, Sutthiruang-wong P, Spick C, Radu C, Weber WA, Tap WD, Eilber FC. 3′-Deoxy-3′-[18F]fluorothymidine positron emission tomography for response assessment in soft tissue sarcoma: A pilot study to correlate imaging findings with tissue thymidine kinase 1 and Ki-67 activity and histopathologic response. Cancer. 2012; 118:3135–3144. [PubMed: 22020872]

Bloom JD, Dutia MD, Johnson BD, Wissner A, Burns MG, Largis EE, Dolan JA, Claus TH. Disodium (R, R)-5-[2-[[2-(3-chloro-phenyl)-2-hydroxyethyl]-amino] propyl]-1,3-benzodioxole-2,2-dicarboxylate (CL-316, 243). A potent beta-adrenergic agonist virtually specific for beta 3 receptors. A promising antidiabetic and antiobsity agent. J Med Chem. 1992; 35:3081–3084. [PubMed: 1354264]

Bronnikov G, Bengtsson T, Kramarova L, Golozoubova V, Cannon B, Nedergaard J. Beta1 to beta3 switch in control of cyclic adenosine monophosphate during brown adipocyte development explains distinct beta-adrenoceptor subtype mediation of proliferation and differentiation. Endocrinology. 1999; 140:4185–4197. [PubMed: 10465291]

Burrows RC, Freeman SD, Charlop AW, Wiseman RW, Adamsen TC, Krohn KA, Spence AM. [18F]-2-fluoro-2-deoxyglucose transport kinetics as a function of extracellular glucose concentration in malignant glioma, fibroblast and macrophage cells in vitro. Nucl Med Biol. 2004; 31:1–9. [PubMed: 14741565]

Bymaster FP, Katner JS, Nelson DL, Hemrick-Luecke SK, Threlkeld PG, Heiligenstein JH, Morin SM, Gehlert DR, Perry KW. Atomoxetine increases extracellular levels of norepinephrine and dopamine in prefrontal cortex of rat: A potential mechanism for efficacy in attention deficit/hyperactivity disorder. Neuropsychopharmacology. 2002; 27:699–711. [PubMed: 12431845]

Cannon B, Nedergaard J. Brown adipose tissue: Function and physiological significance. Physiol Rev. 2004; 84:277–359. [PubMed: 14715917]

Cheng WY, Zhu ZH, Ouyang M. Patterns and characteristics of brown adipose tissue uptake of 18F-FDG positron emission tomograph/computed tomography imaging. Zhongguo Yi Xue Ke Xue Yuan Xue Bao. 2009; 31:370–373. [PubMed: 19621528]

Chernogubova E, Cannon B, Bengtsson T. Norepinephrine increases glucose transport in brown adipocytes via beta3-adreno-ceptors through a cAMP, PKA, and PI3-kinase-dependent pathway stimulating conventional and novel PKCs. Endocrinology. 2004; 145:269–280. [PubMed: 14551227]

Cohade C, Osman M, Pannu HK, Wahl RL. Uptake in supra-clavicular area fat ("USA-Fat"): Description on ^{18}F-FDG PET/CT. J Nucl Med. 2003; 44:170–176. [PubMed: 12571205]

Constantinescu CC, Mukherjee J. Performance evaluation of an Inveon PET preclinical scanner. Phys Med Biol. 2009; 54:2885–2899. [PubMed: 19384008]

Cypess AM, Chen YC, Sze C, Wang K, English J, Chan O, Holman AR, Tal I, Palmer MR, Kolodny GM, Kahn CR. Cold but not sympathomimetics activates human brown adipose tissue in vivo. Proc Natl Acad Sci USA. 2012; 109:10001–10005. [PubMed: 22665804]

Cypess AM, Lehman S, Williams G, Tal I, Rodman D, Goldfine AB, Kuo FC, Palmer EL, Tseng YH, Doria A, Kolodny GM, Kahn CR. Identification and importance of brown adipose tissue in adult humans. N Engl J Med. 2009; 360:1509–1517. [PubMed: 19357406]

Dallner OS, Chernogubova E, Brolinson KA, Bengtsson T. Beta3-adrenergic receptors stimulate glucose uptake in brown adipocytes by two mechanisms independently of glucose transporter 4 translocation. Endocrinology. 2006; 147:5730–5739. [PubMed: 16959848]

De Matteis R, Ricquier D, Cinti S. TH-, NPY-, SP-, and CGRP-immunoreactive nerves in interscapular brown adipose tissue of adult rats acclimated at different temperatures: An immunohistochemical study. J Neurocytol. 1998; 27:877–886. [PubMed: 10659680]

Eng J. Sample size estimation: how many individuals should be studied? Radiology. 2003; 227:309–313. [PubMed: 12732691]

Fueger BJ, Czernin J, Hildebrandt I, Tran C, Halpern BS, Stout D, Phelps ME, Weber WA. Impact of animal handling on the results of 18F-FDG PET studies in mice. J Nucl Med. 2006; 47:999–1006. [PubMed: 16741310]

Gadde KM, Yonish GM, Wagner HR II, Foust MS, Allison DB. Atomoxetine for weight reduction in obese women: A preliminary randomised controlled trial. Int J Obes. 2006; 30:1138–1142.

Garnock-Jones KP, Keating GM. Atomoxetine: A review of its use in attention-deficit hyperactivity disorder in children and adolescents. Paediatr Drugs. 2009; 11:203–226. [PubMed: 19445548]

Habel LA, Cooper WO, Sox CM, Chan KA, Fireman BH, Arbogast PG, Cheetham TC, Quinn VP, Dublin S, Boudreau DM, Andrade SE, Pawloski PA, Raebel MA, Smith DH, Achacoso N, Uratsu C, Go AS, Sidney S, Nguyen-Huynh MN, Ray WA, Selby JV. ADHD medications and risk of serious cardiovascular events in young and middle-aged adults. JAMA. 2011; 306:2673–2683. [PubMed: 22161946]

Hamann A, Flier JS, Lowell BB. Decreased brown fat markedly enhances susceptibility to diet-induced obesity, diabetes, and hyperlipidemia. Endocrinology. 1996; 137:21–29. [PubMed: 8536614]

Hildebrandt IJ, Su H, Weber WA. Anesthesia and other considerations for in vivo imaging of small animals. ILAR J. 2008; 49:17–26. [PubMed: 18172330]

Inokuma K, Ogura-Okamatsu Y, Toda C, Kimura K, Yamashita H, Saito M. Uncoupling protein 1 is necessary for norepinephrine-induced glucose utilization in brown adipose tissue. Diabetes. 2005; 54:1385–1391. [PubMed: 15855324]

Iyer RB, Guo CC, Perrier N. Adrenal pheochromocytoma with surrounding brown fat stimulation. AJR. 2009; 192:300–301. [PubMed: 19098214]

Jacene HA, Cohade CC, Zhang Z, Wahl RL. The relationship between patients' serum glucose levels and metabolically active brown adipose tissue detected by PET/CT. Mol Imaging Biol. 2011; 13:1278–1283. [PubMed: 21140233]

Jensen MD, Haymond MW, Gerich JE, Cryer PE, Miles JM. Lipolysis during fasting. Decreased suppression by insulin and increased stimulation by epinephrine. J Clin Investig. 1987; 79:207–213. [PubMed: 3540009]

Kim S, Krynyckyi BR, Machac J, Kim CK. Temporal relation between temperature change and FDG uptake in brown adipose tissue. Eur J Nucl Med Mol Imaging. 2008; 35:984–989. [PubMed: 18157529]

Kim YW, Shin JC, An YS. Treatment of chronic akinetic mutism with atomoxetine: subtraction analysis of brain f-18 fluorodeoxyglucose positron emission tomographic images before and after medication: A case report. Clin Neuropharmacol. 2010; 33:209–211. [PubMed: 20661027]

Lachance J, Page E. Hormonal factors influencing fat deposition in the interscapular brown adipose tissue of the white rat. Endocrinology. 1953; 52:57–64. [PubMed: 13021112]

Lafontan M, Berlan M. Fat cell adrenergic receptors and the control of white and brown fat cell function. J Lipid Res. 1993; 34:1057–1091. [PubMed: 8371057]

Ledbetter M. Atomoxetine: A novel treatment for child and adult ADHD. Neuropsychiatr Dis Treat. 2006; 2:455–466. [PubMed: 19412494]

Lee KH, Ko BH, Paik JY, Jung KH, Choe YS, Choi Y, Kim BT. Effects of anesthetic agents and fasting duration on 18F-FDG biodistribution and insulin levels in tumor-bearing mice. J Nucl Med. 2005; 46:1531–1536. [PubMed: 16157537]

Letovanec I, Allenbach G, Mihaescu A, Nicod Lalonde M, Schmidt S, Stupp R, Fitting JW, Boubaker A, Ris HB, Prior JO. 18F-fluorodeoxyglucose PET/CT findings in pleural effusions of patients with known cancer. A cytopathological correlation. Nuklearmedizin. 2012; 51:186–193. [PubMed: 22584348]

Lin SF, Fan X, Yeckel CW, Weinzimmer D, Mulnix T, Gallezot JD, Carson RE, Sherwin RS, Ding YS. Ex vivo and in vivo Evaluation of the norepinephrine transporter ligand [(11)C]MRB for brown adipose tissue imaging. Nucl Med Biol. 2012; 39:1081–1086. [PubMed: 22595487]

Liu X, Perusse F, Bukowiecki LJ. Mechanisms of the antidiabetic effects of the beta 3-adrenergic agonist CL-316 243 in obese Zucker-ZDF rats. Am J Physiol. 1998; 274(5 Pt 2):R1212–R1219. [PubMed: 9644032]

Ma SW, Foster DO. Uptake of glucose and release of fatty acids and glycerol by rat brown adipose tissue in vivo. Can J Physiol Pharmacol. 1986; 64:609–614. [PubMed: 3730946]

Marette A, Bukowiecki LJ. Noradrenaline stimulates glucose transport in rat brown adipocytes by activating thermogenesis. Evidence that fatty acid activation of mitochondrial respiration enhances glucose transport. Biochem J. 1991; 277(Pt 1):119–124. [PubMed: 1713031]

Marnane M, Merwick A, Sheehan OC, Hannon N, Foran P, Grant T, Dolan E, Moroney J, Murphy S, O'Rourke K, O'Malley K, O'Donohoe M, McDonnell C, Noone I, Barry M, Crowe M, Kavanagh E, O'Connell M, Kelly PJ. Carotid plaque inflammation on 18F-fluorodeoxyglucose positron emission tomography predicts early stroke recurrence. Ann Neurol. 2012; 71:709–718. [PubMed: 22461139]

Mattsson CL, Csikasz RI, Chernogubova E, Yamamoto DL, Hogberg HT, Amri EZ, Hutchinson DS, Bengtsson T. Beta(1)-adrenergic receptors increase UCP1 in human MADS brown adipocytes and rescue cold-acclimated beta(3)-adrenergic receptor-knockout mice via nonshivering thermogenesis. Am J Physiol. 2011; 301:E1108–E1118.

McElroy SL, Guerdjikova A, Kotwal R, Welge JA, Nelson EB, Lake KA, Keck PE Jr, Hudson JI. Atomoxetine in the treatment of binge-eating disorder: A randomized placebo-controlled trial. J Clin Psychiatry. 2007; 68:390–398. [PubMed: 17388708]

Michelson D, Adler L, Spencer T, Reimherr FW, West SA, Allen AJ, Kelsey D, Wernicke J, Dietrich A, Milton D. Atomoxetine in adults with ADHD: Two randomized, placebo-controlled studies. Biol Psychiatry. 2003; 53:112–120. [PubMed: 12547466]

Mirbolooki MR, Constantinescu CC, Pan ML, Mukherjee J. Quantitative assessment of brown adipose tissue metabolic activity and volume using 18F-FDG PET/CT and β 3-adrenergic receptor activation. EJNMMI Res. 2011; 1:30. [PubMed: 22214183]

Mizuma H, Shukuri M, Hayashi T, Watanabe Y, Onoe H. Establishment of in vivo brain imaging method in conscious mice. J Nucl Med. 2010; 51:1068–1075. [PubMed: 20554730]

Mukherjee J, Yang ZY, Lew R, Brown T, Kronmal S, Cooper MD, Seiden LS. Evaluation of d-amphetamine effects on the binding of dopamine D-2 receptor radioligand, 18F-fallypride in nonhuman primates using positron emission tomography. Synapse (New York, NY). 1997; 27:1–13.

Nedergaard J, Bengtsson T, Cannon B. Unexpected evidence for active brown adipose tissue in adult humans. Am J Physiol. 2007; 293:E444–E452.

Nedergaard J, Bengtsson T, Cannon B. Three years with adult human brown adipose tissue. Ann N Y Acad Sci. 2010; 1212:E20–E36. [PubMed: 21375707]

Nedergaard J, Bengtsson T, Cannon B. New powers of brown fat: Fighting the metabolic syndrome. Cell Metab. 2011; 13:238–240. [PubMed: 21356513]

Pfannenberg C, Werner MK, Ripkens S, Stef I, Deckert A, Schmadl M, Reimold M, Haring HU, Claussen CD, Stefan N. Impact of age on the relationships of brown adipose tissue with sex and adiposity in humans. Diabetes. 2010; 59:1789–1793. [PubMed: 20357363]

Postic C, Leturque A, Printz RL, Maulard P, Loizeau M, Granner DK, Girard J. Development and regulation of glucose transporter and hexokinase expression in rat. Am J Physiol. 1994; 266(4 Pt 1):E548–E559. [PubMed: 8178975]

Quevedo S, Roca P, Pico C, Palou A. Sex-associated differences in cold-induced UCP1 synthesis in rodent brown adipose tissue. Pflugers Arch. 1998; 436:689–695. [PubMed: 9716701]

Roe K, Aleksandersen TB, Kristian A, Nilsen LB, Seierstad T, Qu H, Ree AH, Olsen DR, Malinen E. Preclinical dynamic 18F-FDG PET: Tumor characterization and radiotherapy response assessment by kinetic compartment analysis. Acta Oncol (Stock-holm, Sweden). 2010; 49:914–921.

Rosler M, Casas M, Konofal E, Buitelaar J. Attention deficit hyperactivity disorder in adults. World J Biol Psychiatry. 2010; 11:684–698. [PubMed: 20521876]

Saito M, Okamatsu-Ogura Y, Matsushita M, Watanabe K, Yoneshiro T, Nio-Kobayashi J, Iwanaga T, Miyagawa M, Kameya T, Nakada K, Kawai Y, Tsujisaki M. High incidence of metabolically active brown adipose tissue in healthy adult humans: Effects of cold exposure and adiposity. Diabetes. 2009; 58:1526–1531. [PubMed: 19401428]

Santalucia T, Camps M, Castello A, Munoz P, Nuel A, Testar X, Palacin M, Zorzano A. Developmental regulation of GLUT-1 (erythroid/Hep G2) and GLUT-4 (muscle/fat) glucose transporter expression in rat heart, skeletal muscle, and brown adipose tissue. Endocrinology. 1992; 130:837–846. [PubMed: 1370797]

Sauer JM, Ring BJ, Witcher JW. Clinical pharmacokinetics of atomoxetine. Clin Pharmacokinet. 2005; 44:571–590. [PubMed: 15910008]

Scheen AJ. Cardiovascular risk-benefit profile of sibutramine. Am J Cardiovasc Drugs. 2010; 10:321–334. [PubMed: 20860415]

Scherer D, Hassel D, Bloehs R, Zitron E, von Lowenstern K, Seyler C, Thomas D, Konrad F, Burgers HF, Seemann G, Rottbauer W, Katus HA, Karle CA, Scholz EP. Selective noradrenaline reuptake inhibitor atomoxetine directly blocks hERG currents. Br J Pharmacol. 2009; 156:226–236. [PubMed: 19154426]

Schinagl DA, Span PN, Oyen WJ, Kaanders JH. Can FDG PET predict radiation treatment outcome in head and neck cancer? Results of a prospective study. Eur J Nucl Med Mol Imaging. 2011; 38:1449–1458. [PubMed: 21461734]

Shimizu Y, Satoh S, Yano H, Minokoshi Y, Cushman SW, Shimazu T. Effects of noradrenaline on the cell-surface glucose transporters in cultured brown adipocytes: Novel mechanism for selective activation of GLUT1 glucose transporters. Biochem J. 1998; 330(Pt 1):397–403. [PubMed: 9461536]

Stefan N, Pfannenberg C, Haring HU. The importance of brown adipose tissue. N Engl J Med. 2009; 361:416–417. author reply 418–421. [PubMed: 19630141]

Symonds ME, Budge H, Perkins AC, Lomax MA. Adipose tissue development: impact of the early life environment. Prog Biophys Mol Biol. 2011; 106:300–306. [PubMed: 21163289]

van Marken Lichtenbelt WD, Vanhommerig JW, Smulders NM, Drossaerts JM, Kemerink GJ, Bouvy ND, Schrauwen P, Teule GJ. Cold-activated brown adipose tissue in healthy men. N Engl J Med. 2009; 360:1500–1508. [PubMed: 19357405]

Vanttinen M, Nuutila P, Kuulasmaa T, Pihlajamaki J, Hallsten K, Virtanen KA, Lautamaki R, Peltoniemi P, Takala T, Viljanen AP, Knuuti J, Laakso M. Single nucleotide polymorphisms in the peroxisome proliferator-activated receptor delta gene are associated with skeletal muscle glucose uptake. Diabetes. 2005; 54:3587–3591. [PubMed: 16306381]

Virtanen KA, Lidell ME, Orava J, Heglind M, Westergren R, Niemi T, Taittonen M, Laine J, Savisto NJ, Enerback S, Nuutila P. Functional brown adipose tissue in healthy adults. N Engl J Med. 2009; 360:1518–1525. [PubMed: 19357407]

Weyer C, Tataranni PA, Snitker S, Danforth E Jr, Ravussin E. Increase in insulin action and fat oxidation after treatment with CL 316, 243, a highly selective beta3-adrenoceptor agonist in humans. Diabetes. 1998; 47:1555–1561. [PubMed: 9753292]

Yamaga LY, Thom AF, Wagner J, Baroni RH, Hidal JT, Funari MG. The effect of catecholamines on the glucose uptake in brown adipose tissue demonstrated by (18)F-FDG PET/CT in a patient with adrenal pheochromocytoma. Eur J Nucl Med Mol Imaging. 2008; 35:446–447. [PubMed: 17909796]

Yoneshiro T, Aita S, Matsushita M, Okamatsu-Ogura Y, Kameya T, Kawai Y, Miyagawa M, Tsujisaki M, Saito M. Age-related decrease in cold-activated brown adipose tissue and accumulation of body fat in healthy humans. Obesity (Silver Spring). 2011; 19:1755–1760. [PubMed: 21566561]

Yoshida T, Sakane N, Wakabayashi Y, Umekawa T, Kondo M. Anti-obesity and anti-diabetic effects of CL 316, 243, a highly specific beta 3-adrenoceptor agonist, in yellow KK mice. Life Sci. 1994; 54:491–498. [PubMed: 8309351]

Zelinka T, Petrak O, Turkova H, Holaj R, Strauch B, Krsek M, Vrankova AB, Musil Z, Duskova J, Kubinyi J, Michalsky D, Novak K, Widimsky J. High incidence of cardiovascular complications in pheochromocytoma. Horm Metab Res. 2012; 44:379–384. [PubMed: 22517556]

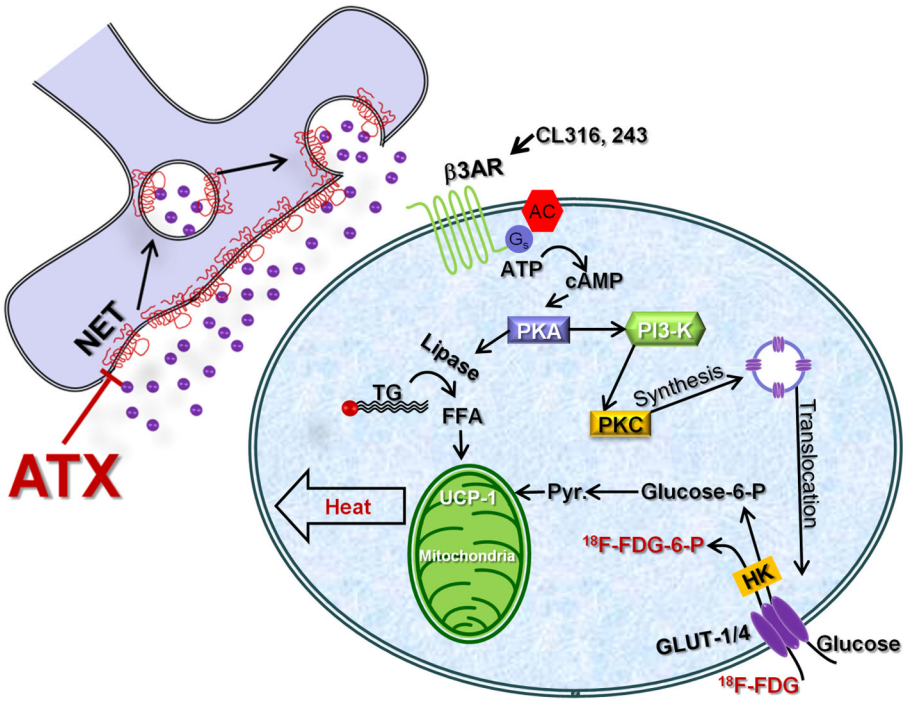

Fig. 1.

Schematic showing the mechanism of glucose uptake in a brown adipocyte. Aomoxetine (ATX) inhibits norepinephrine reuptake by blocking presynaptic norepinephrine transporter (NET), which results in a longer activation of postsynaptic β-adrenergic receptor. CL-316, 243 (CL) activate β_3-adrenergic receptor (β_3AR) directly. Production of cyclic adenosine monophosphate (cAMP) and protein kinase A (PKA) trigger lipase and hydrolysis of triglycerides in one hand. On the other hand, it phosphorylates phosphoinositide-3-kinase (PI3 K) followed by a series of reactions resulting in synthesis and translocation of GLUT 1/4, and overexpression of hexokinase (HK), which leads to an increase in glucose and ^{18}F-FDG uptake. ●, Norepinephrine; PKC, protein kinase C; Pyr,: pyruvate; UCP-1, uncoupling protein-1.

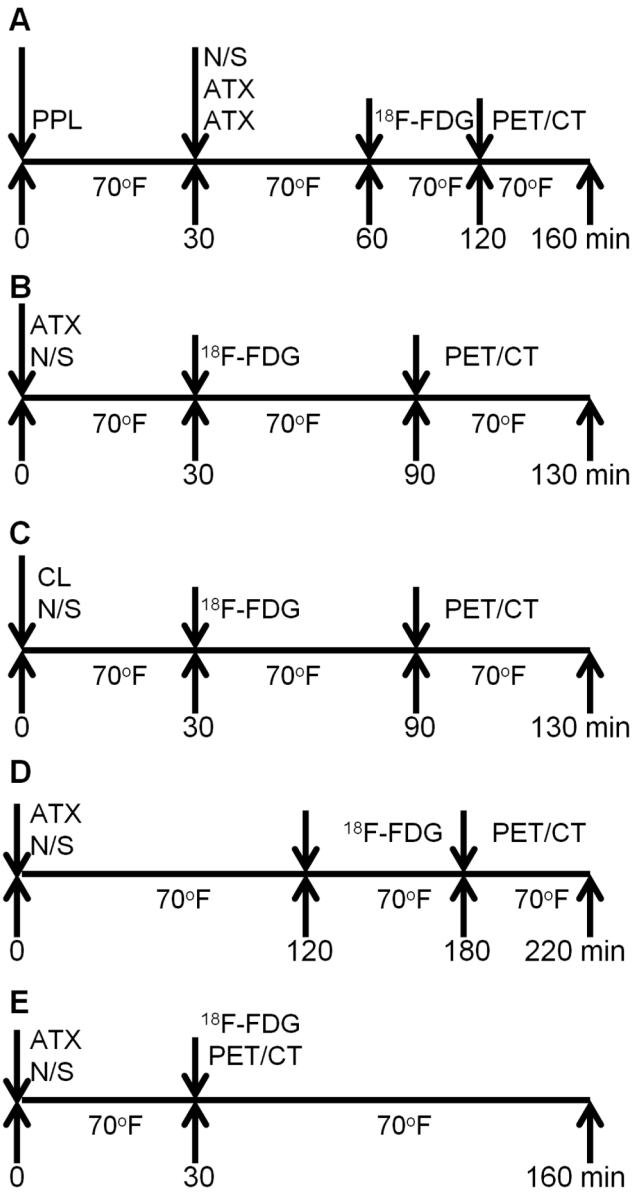

Fig. 2.

Study protocols: All rats were kept awake in room temperature for additional 60 min prior to 30 min PET acquisition followed by 10 min CT acquisition for attenuation correction and anatomical delineation of PET images. **A:** Fasted rats were injected with either atomoxetine (ATX) or normal saline (N/S) 30 min prior to ^{18}F-FDG administration. Propranolol (PPL) was given, intraperitoneally, 30 min prior to ATX administration ($n = 3$). **B:** Non-fasted rats were injected with either ATX or N/S saline 30 min prior to ^{18}F-FDG administration ($n = 3$). **C:** Non-fasted rats were injected with either CL-316, 243 (CL) or N/S 30 min prior to ^{18}F-FDG administration ($n = 3$). **D**: Non-fasted rats were injected with either ATX or N/S 120 min prior to ^{18}F-FDG administration ($n = 3$). **E:** Fasted rats were injected with either atomoxetine (ATX) or normal saline (N/S) 30 min prior to dynamic PET imaging ($n = 3$).

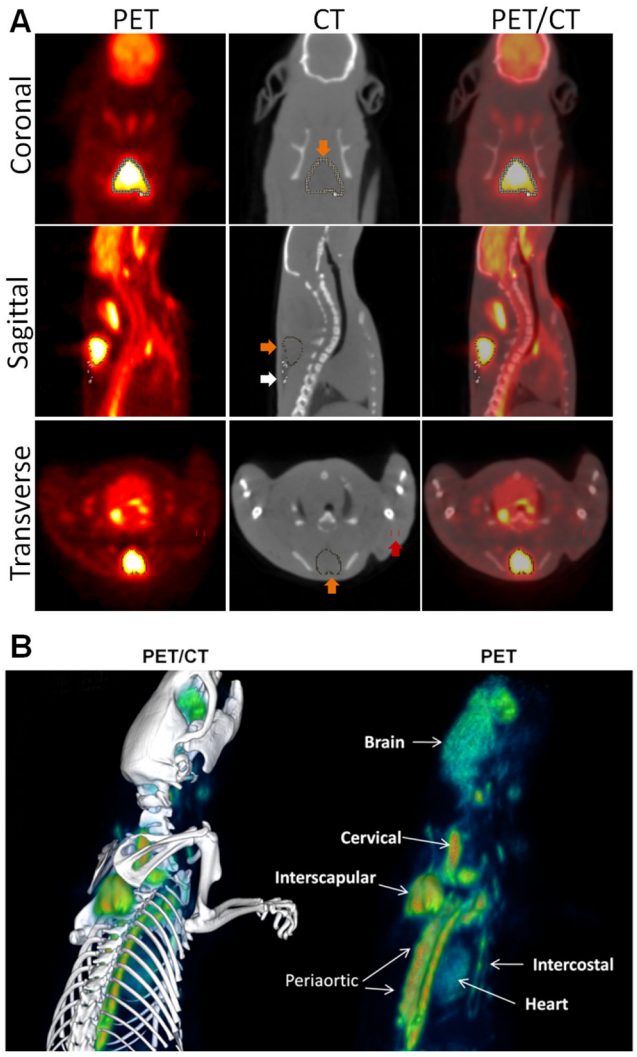

Fig. 3.

A: Coronal, sagittal, and transverse views of PET/CT images showing how automatic contour volumes of interest (VOI) were drawn on the atomoxetine-activated IBAT, surrounding IWAT and muscle (biceps): PET (left), CT (middle), and fused PET/CT (right). Color of the arrows: brown: brown adipose tissue; white: white adipose tissue; and red: muscle. **B:** Three dimensional analysis of PET (right) and PET/CT (left) images clearly show interscapular, cervical, periaortic, and intercostal BATs.

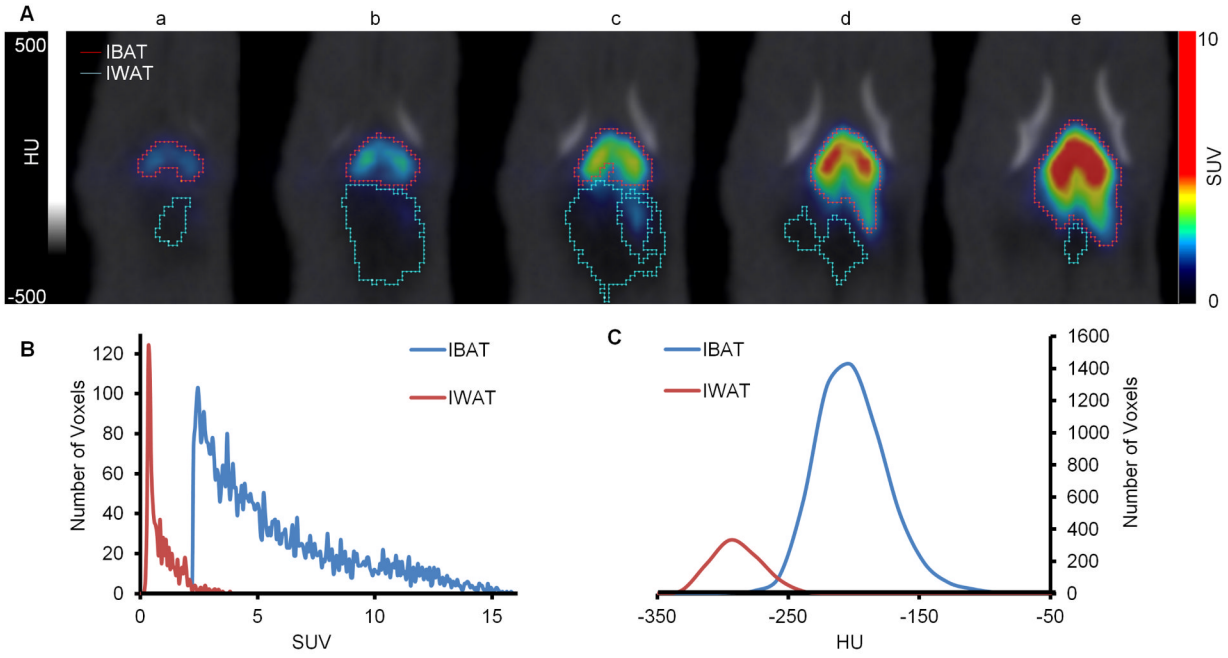

Fig. 4.

A: Coronal views of sequentially co-registered PET/CT images showing how automatic contours of volumes of interest (VOI) were drawn on the IBAT and IWAT of atomoxetine-treated rats. **A–E:** Sequential slices from top to bottom of IWAT. B: Differences of the IBAT and IWAT VOIs based on PET data (SUV). C: Differences of the IBAT and IWAT VOIs based on CT data (Hounsfield Unit).

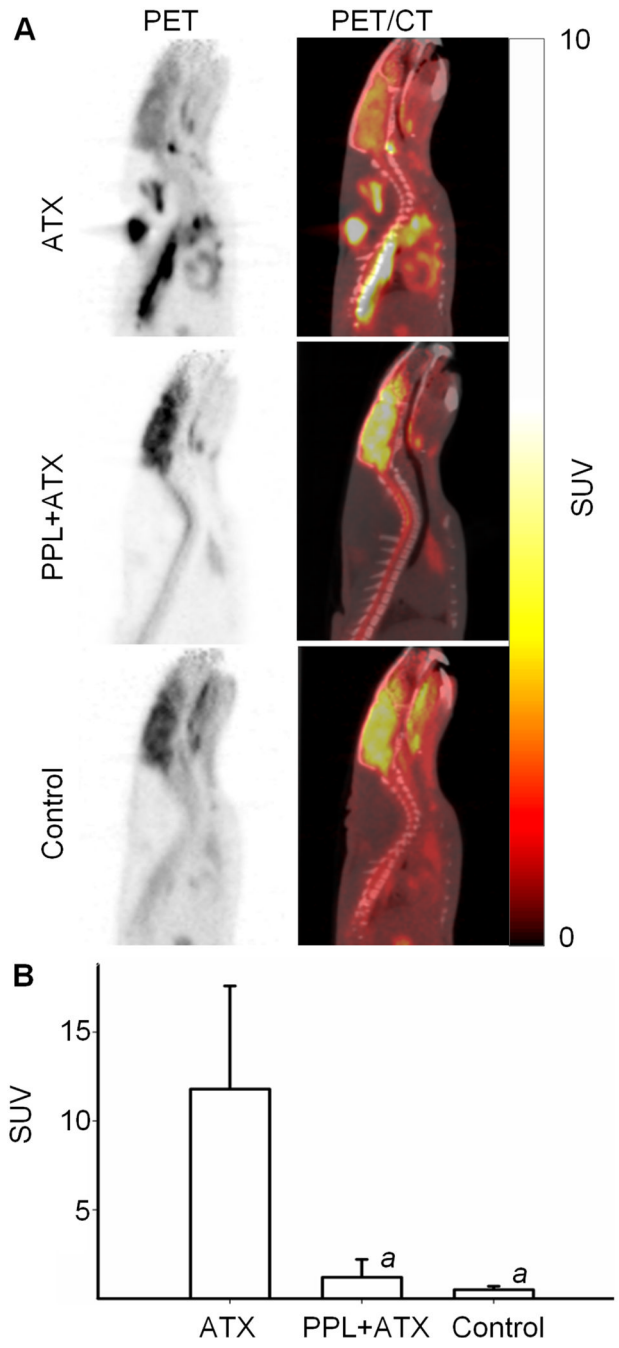

Fig. 5.

Sagittal views of PET/CT images in fasted rats: **A:** PET (left), and fused PET/CT (right) show intense ^{18}F-FDG uptake in the atomoxetine-activated (ATX) BAT, but faint uptakes in the control and the atomoxetine-propranolol (PPL + ATX) treated group. **B:** Quantitative analysis of PET/CT images for intercostal BAT uptake in three studied groups. Data are mean ± SD; $^{a}P < 0.001$ when compared with ATX; same animals ($n = 3$) were scanned under different experimental conditions.

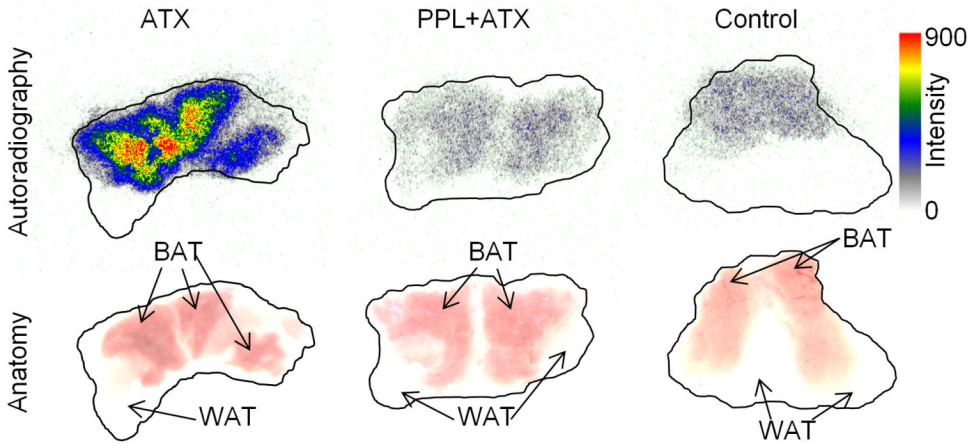

Fig. 6.

Ex-vivo ^{18}F-FDG autoradiography (upper row) shows intense uptake in the IBAT of atomoxetine (ATX) treated group (Left) when compared with atomoxetine-propranolol (PPL + ATX) treated group (Middle) and control (left). Consecutive sections of autoradiographic images (Lower row) show IBAT tissue and the surrounding white adipose tissues marked by arrows (n = 3, each group).

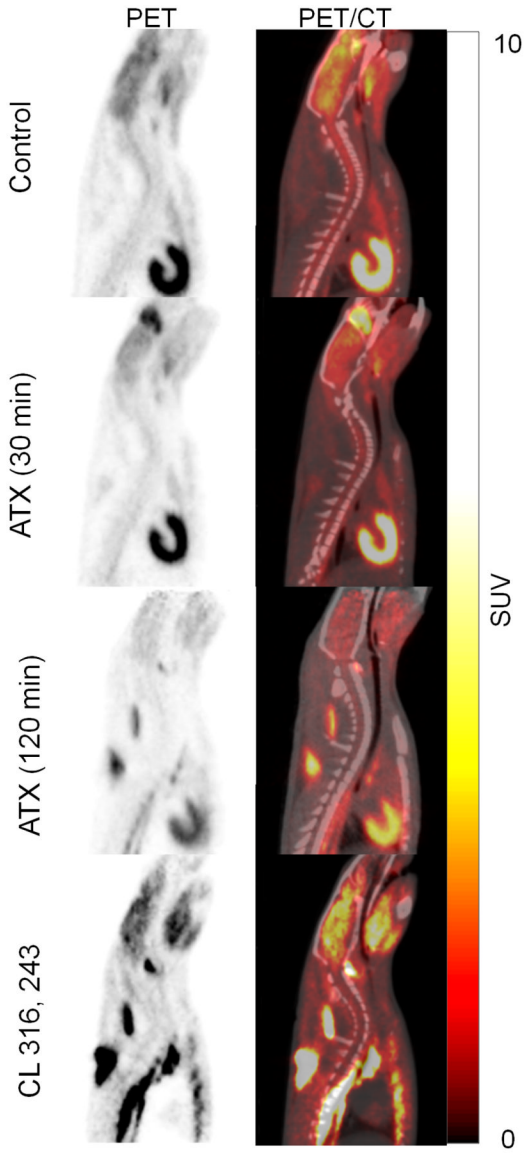

Fig. 7.

Sagittal views of PET/CT images in non-fasted rats: PET (left), and fused PET/CT (right) show faint ^{18}F-FDG uptake in the control and atomoxetine-activated BAT, when it was administered 30 min after atomoxetine injection, ATX (30 min); augmented ^{18}F-FDG uptake when it was administered 120 min after ATX injection, ATX (120 min); and intense ^{18}F-FDG uptake in the CL-316, 243-activated BAT. Same animals (n = 3) were scanned under different experimental conditions.

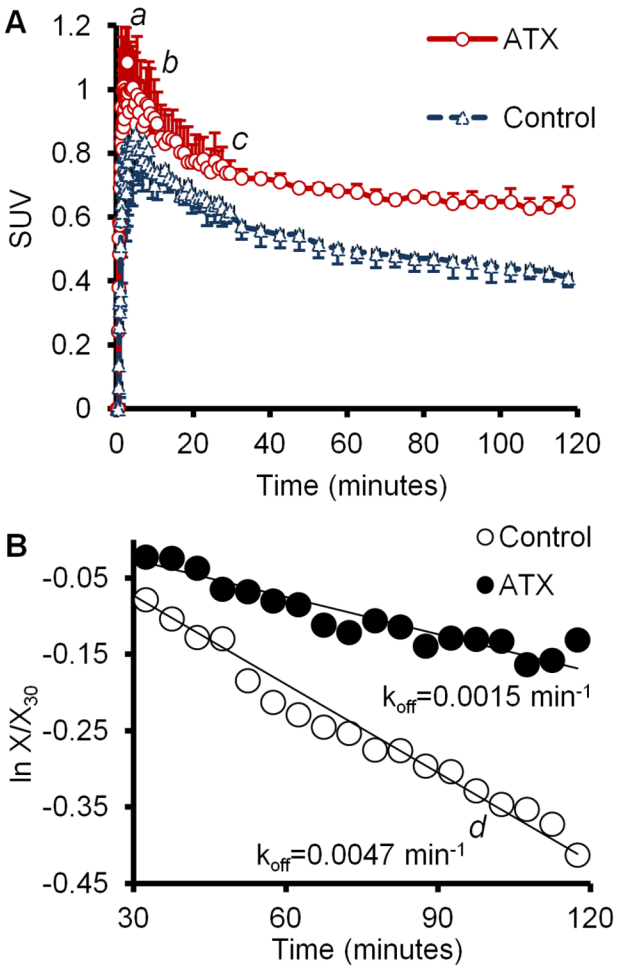

Fig. 8.

A: Time activity curves of ^{18}F-FDG SUV in IBAT of atomoxetine-treated when compared with untreated rats (a: t_{2min}, $P = 0.018$; b: t_{10min}, $P = 0.040$; c: t_{30min}, $P = 0.012$). B: Plot of ln $X/X30$ ($X30$ is ^{18}F-FDG SUV at 30 min and X is ^{18}F-FDG SUV at various times post-$X30$) vs. time shows clearance rate of 18F-FDG from IBAT in the absence and at the presence of atomoxetine.

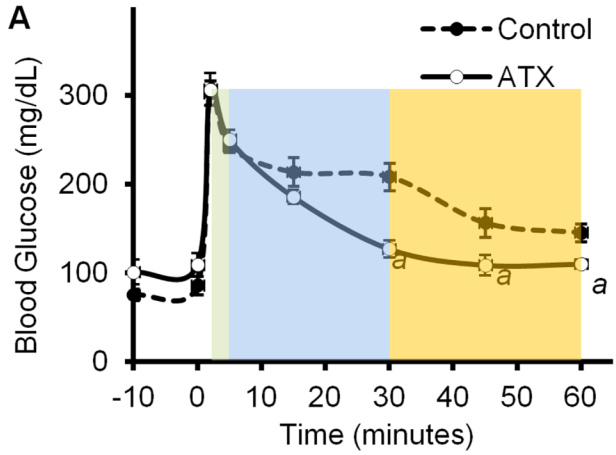

B

	ATX	Control	*P* value
Phase 1	5.9±1.8[b]	6.4±2.4	p<0.8
Phase 2	1.9±0.3	0.6±0.4	p<0.001
Phase 3	0.4±0.3	0.9±0.3	p<0.1

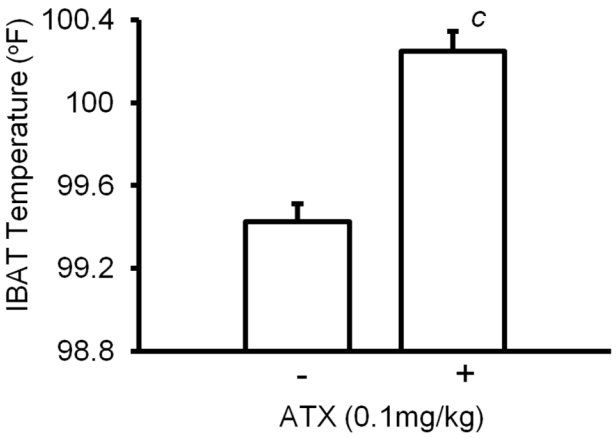

Fig. 9.

Functional effects of atomoxetine: **A:** glucose concentrations of blood samples collected during the intravenous glucose tolerance test (IVGTT; [a]P < 0.005). **B:** Blood glucose clearance rate during three different phases of intravenous glucose tolerance: Phase 1: fast clearance (minutes 2–5); phase 2: moderate clearance (minutes 5–30); phase 3: slow clearance (minutes 30–60) using the following formula: $G_c = \frac{(G_{t1} - G_{t0})}{G_{t0} \times (t1 - t_0)}$ where G_{t0} is blood glucose level at the beginning of the phase; G_{t1} is blood glucose level at the end of the phase; $t0$ is time when the phase begins; and $t1$ is time when the phase ends. [b]Mean ± SD (% min^{-1}). **C:** IBAT temperature before and 60 min after atomoxetine (ATX) injection ([c]P < 0.01). Same animals (n = 4) were studied under different experimental conditions.

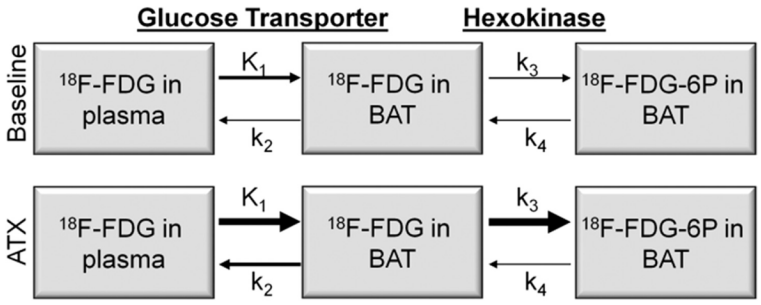

Fig. 10.
Schematic expression of a 2-compartment model for ^{18}F-FDG kinetics.

TABLE I

^{18}F-FDG uptake of interscapular white adipose tissue (IWAT) and muscle (biceps) in three studied groups when the rats were fasted

	ATX	PPL + ATX	Control
IWAT	0.8 ± 0.2	0.5 ± 0.1	0.3 ± 0.1[a]
Muscle	0.3 ± 0.04	0.3 ± 0.03	0.3 ± 0.05

ATX: atomoxetine; PPL: propranolol.

[a]Mean ± SD, SUV, $P < 0.05$ when compared with ATX, same animals ($n = 3$) were scanned under different experimental conditions.

TABLE II

Autoradiography measures of ^{18}F-FDG uptake in transverse sections of interscapular brown adipose tissue (IBAT) and the surrounding white adipose tissue (IWAT)

Groups	IBAT	IWAT	Ratio[a]
ATX	12.5 ± 0.7[bcd]	0.2 ± 0.05	67.8 ± 15.8[c]
PPL + ATX	2.8 ± 0.2[cd]	0.2 ± 0.08	27.7 ± 5.3[c]
Control	2.0 ± 0.2[d]	0.08 ± 0.02	18.4 ± 9.0

ATX: atomoxetine; PPL: propranolol.

[a] Ratio: IBAT/IWAT ratio.

[b] Mean ± SD × 10^6 DLU/mm^2, $n = 3$.

[c] $P < 0.05$ when compared with control.

[d] $P < 0.05$ when compared with WAT.

TABLE III

^{18}F-FDG uptake of interscapular white adipose tissue (IWAT) and muscle (biceps) with and without atomoxetine treatment when the rats were nonfasted

	ATX (120 min)	ATX (30 min)	Control	*P*-value
IWAT	0.4 ± 0.2[a]	0.5 ± 0.2	0.5 ± 0.1	$P < 0.7$
Muscle	0.4 ± 0.1	0.6 ± 0.2	0.7 ± 0.2	$P < 0.8$

ATX (30 min): ^{18}F-FDG was administered 30 min after atomoxetine injection; ATX (120 min): ^{18}F-FDG was administered 120 min after ATX injection.

[a]Mean ± SD (SUV); same animals ($n = 3$) were scanned under different experimental conditions.